



NUMERICAL AND EXPERIMENTAL ANALYSIS OF NATURAL CONVECTION HEAT TRANSFER IN AN ARRAY OF VERTICAL CHANNELS WITH TWO-DIMENSIONAL PROTRUDING HEAT SOURCES

Ana Cristina Avelar

Universidade Estadual de Campinas, Faculdade de Engenharia Mecânica, Depto de Energia
Cx. P. 6122 – 13083-970 – e-mail:crisibj@uol.com.br

Marcelo Moreira Ganzarolli

Universidade Estadual de Campinas, Faculdade de Engenharia Mecânica, Depto. de Energia
Cx. P. 6122 – 13083-970 – e-mail:ganza@fem.unicamp.br

Abstract. Natural convection heat transfer from an array of vertical, parallel plates, forming open channels containing heated protruding elements attached to one of the walls, is analyzed both numerically and experimentally. An experimental setup was built consisting of five fiberglass plates, with seven aluminum protrusions mounted in one of the plate surfaces, accommodated in a metallic structure that allows variation of the distance between plates. It is analyzed the situation of uniform heating of the plates, with variation of the distance between plates and the power dissipated per plate. In the numerical analysis it was used the SIMPLEC algorithm for solving the pressure-velocity coupling. Heat conduction to the walls was also considered and the Navier-Stokes equations were solved in elliptic form. Numerical and experimental results were compared and good agreement was observed.

Keywords. Natural Convection, Protruding Heat Sources, Vertical Channels

1. INTRODUCTION

Natural convection heat transfer in vertical channels has been intensively investigated in the last decades because of its application in the cooling of electronic equipment operating at low heat dissipation rates. The main advantage of natural convection is its simplicity and reliability, because the air movement is simply generated by local density gradients in the presence of the gravitational field. The literature on natural convection in open vertical channels is extensive.

The first work was attributed to Elenbaas (1942). He established overall heat transfer correlations for isothermal channels over a wide range of thermal and geometric parameters. For the case of channels with smooth plates, this problem has been studied for several types of boundary conditions imposed at the channel walls, such as uniformly symmetric or asymmetric heated plates, one plate insulated and the other with a discrete heated section, and two discrete heated plates. Many of them were reviewed by Incropera (1988), and by Peterson and Ortega (1990), who carried out comprehensive reviews on thermal control of electronic equipment. There are also several works dealing with channels with multiple protruding heat sources, mainly in the last decade. Most of them are about plates with few heat sources, 1 to 3, or with protrusions densely distributed. Free convection flows in vertical channels with two rectangular obstructions on opposite walls was studied numerically by Viswamula and Amin (1994). Four different geometry's were employed to study the effect of the parameters like Rayleigh number, aspect ratio and obstruction locations on the average Nusselt number. Fujii et al (1996) analyzed numerical and experimentally the natural

convection heat transfer to air from an array of vertical parallel plates with protruding discrete and densely distributed heat sources. Behnia and Nakayama (1998) performed numerical simulations on

natural convection considering the same geometry analyzed by Fujii et al (1996), but the analysis was performed for several values of plate thermal conductivity and channel width. Bessaih and Kadja (2000) performed numerical simulations on turbulent natural convection cooling of three identical heated ceramic components mounted on a vertical adiabatic channel wall. It was investigated the effect on cooling of the spacing between components and of the removal of heat input in one of the components.

The present work is aimed at investigating the conjugated problem of natural convection-conduction in an array of vertical channels with two-dimensional heat sources mounted in one of the plate surfaces. The sources are sparsely distributed. It was analyzed the situation of uniform heating of the plates. Numerical solutions are obtained to the full elliptic two-dimensional steady state Navier-Stokes equations using the SIMPLEC algorithm. It was varied the distance between plates and total power dissipated per plate. Experimental temperature measurements were carried out to validate the numerical results. Good agreement was observed between numerical and experimental results.

2. NUMERICAL ANALYSIS

Figure (1) shows the physical model and coordinate system. An infinite number of plates is placed in a vertical parallel arrangement with equal spacing d . Each plate has the same height l and thickness b . On one surface of the plates are mounted seven two-dimensional protruding heat sources separated by the distance s_p . Each heat source has the same dimensions. The total heat generation in each plate is set the same. The solution domain is chosen to be the region bounded by the broken line in Figure (1).

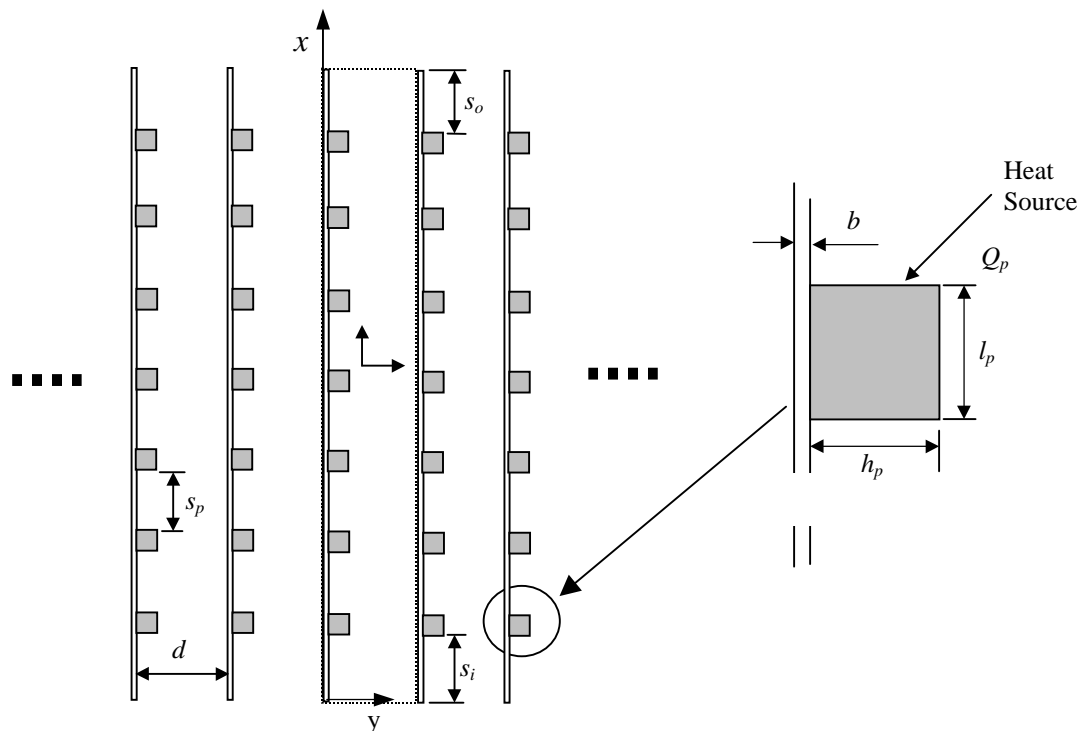


Figure 1 - Physical model and coordinate system.

The flow is assumed to be at steady state, laminar and two-dimensional. The air thermo-physical properties are assumed to remain constant, except for the density in the buoyancy term of the momentum equation, which is assumed to follow the Boussinesq approximation. The heat conduction in the plates and in the heat sources is taken into account. It is admitted uniform heat generation within the heat sources. The radiative heat transfer among the plates and the ambient is not accounted. The problem is analyzed for the situations of uniform heating of the plates. The governing equations are expressed in dimensionless form as follow:

Continuity equation

$$\frac{\partial U}{\partial X} + \frac{\partial V}{\partial Y} = 0 \quad (1)$$

Momentum equation in X direction

$$U \frac{\partial U}{\partial X} + V \frac{\partial V}{\partial Y} = -\frac{\partial P}{\partial Y} + \left(\frac{\text{Pr}}{\text{Ra}}\right)^{1/2} \left(\frac{\partial^2 U}{\partial X^2} + \frac{\partial^2 U}{\partial Y^2}\right) + \theta \quad (2)$$

Momentum equation in Y direction

$$U \frac{\partial V}{\partial X} + V \frac{\partial V}{\partial Y} = -\frac{\partial P}{\partial Y} + \left(\frac{\text{Pr}}{\text{Ra}}\right)^{1/2} \left(\frac{\partial^2 V}{\partial X^2} + \frac{\partial^2 V}{\partial Y^2}\right) \quad (3)$$

A unique form is used to express the energy equation in the fluid and the solid regions

$$U \frac{\partial \theta}{\partial X} + V \frac{\partial \theta}{\partial Y} = (\text{Pr Ra})^{-1/2} \frac{k_i}{k_{\text{air}}} \left(\frac{\partial^2 \theta}{\partial X^2} + \frac{\partial^2 \theta}{\partial Y^2}\right) + f \frac{2L(\text{Pr Ra})^{-1/2}}{npH_p L_p} \quad (4)$$

where:

- $f=1$ for the protruding heat sources and $f=0$ for the rest of the domain;
- k_i is thermal conductivity of the correspondent region. $i=1,2$ and 3 , for air plate and heating sources, respectively;
- np is the number of heated sources.

The boundary conditions are:

Channel entrance ($X = 0$)

$$\theta = V = 0; P = -0.5U_m^2$$

Channel Walls ($Y = 0$ and $Y = B + 1$)

$$U = V = 0$$

A periodic boundary condition is imposed with respect to the temperature at the plate surface, i.e

$$\theta(X,0) = \theta(X,B+1)$$

Channel exit ($Y = l/d$)

$$\frac{\partial U}{\partial X} = \frac{\partial V}{\partial X} = \frac{\partial \theta}{\partial X} = P = 0$$

The pressure values at the channel entrance and exit were obtained from potential flow theory. The dimensionless variables in the above equations are defined by

$$X = \frac{x}{d}, \quad Y = \frac{y}{d}, \quad L = \frac{1}{d}, \quad B = \frac{b}{d}, \quad H_p = \frac{h_p}{d}, \quad L_p = \frac{l_p}{d},$$

$$\theta = \frac{T - T_i}{q'' d / k_{\text{air}}}, \quad U = \frac{u}{u_o}, \quad V = \frac{v}{u_o}, \quad P = \frac{p - p_h}{\rho u_o^2}$$

$$Ra = \frac{q''qd^4\beta}{k_f v_f \alpha_f}, \quad Pr = \frac{v}{\alpha}$$

where q'' is defined based on the total surface area of the plate as

$$q'' = \frac{Q}{2A} = \frac{Q}{2Lw} \quad (5)$$

and the reference velocity, u_o is defined by

$$u_o = \left(d^2 g \beta \frac{q''}{k_{air}} \right)^{1/2} \quad (6)$$

The governing equations were discretized using the control volume formulation described by Patankar (1980), where velocity control volume are staggered with respect to the pressure and temperature control volumes. Coupling of the pressure and velocity fields was treated using the SIMPLEC algorithm (Van Doormal and Rathby, 1984), with the Power-law scheme. The conjugate problem of conduction and convection was dealt by using the harmonic averaging thermal conductivity at the interfaces solid-fluid Patankar (1980). The periodic boundary condition imposed with respect to the temperature at the plate surface was handled by using the CTDMA algorithm (Cyclic TriDiagonal Matrix Algorithm), Patankar et al (1977) to solve the discretized energy equation. No specification of the wall temperature is required in this formulation. This hypothesis was considered to be valid because the measured longitudinal temperature (x direction) in the inner three plates are almost the same, the maximum difference is about 3%. Negligible contact resistance between heat source and plate was assumed. This hypothesis was considered because experimental measurements showed that the temperature difference between the protrusions top surface and base is very small. The equations were solved in a non-uniform grid crowded near the solid walls. The number of nodes was varied from 622~56 to 622~64, depending on the distance between plates. The grid distributions were determined by successive refinements of an initial 312~26 grid until the maximum temperature in the plate changed less than 1%. The convergence of the iterative procedure was tested by the following criterion

$$\frac{|\Gamma_{i,j}^n - \Gamma_{i,j}^{n-1}|_{\max}}{|\Gamma_{i,j}^n|_{\max}} \leq 5 \times 10^{-6} \quad (7)$$

where Γ stands for U , V , θ and the maximum residual in the continuity equation.

3. EXPERIMENTAL ANALISYS

An array of five fiber glass plates was accommodated in a metallic structure that is used in telecommunications devices and that allows variation of the distance between plates. A schematic view of the experimental apparatus is showed in Fig. (2). The plates are numbered from 1 to 5 for convenience.

The structure was maintained about 1m from the ground and placed in a quiet room. Each plate was 365mm heighth (l) and 340mm width (w), with 1,5mm thickness and it had seven heat sources mounted on its surface. The protruding heat sources were constructed from two aluminum bars 12,25mm height, 340mm width and 6,13mm thickness, with one resistance wire between them. The elements resulted were screwed into the fiber glass plates and an equal spacing of 34,5mm was adopted. The protruding heat sources were connected in a way that any desired power level could be set to any given element, independently of the others. Power was supplied to the plates by regulated D.C. sources and both sides of the channels were closed to prevent lateral air flowing. In

order to reduce the radiation heat transfer influence, the heat sources were polished with diamond paste.

Temperature measurements were obtained by using calibrated thermocouples 36 AWG type J, a switch and a digital thermometer. Special care was taken to embed the thermocouples in the aluminum and in the fiber glass surfaces. A very small hole was drilled in their surfaces, which was covered with a thin layer of thermal paste, and the thermocouples were fixed with epoxy adhesive.

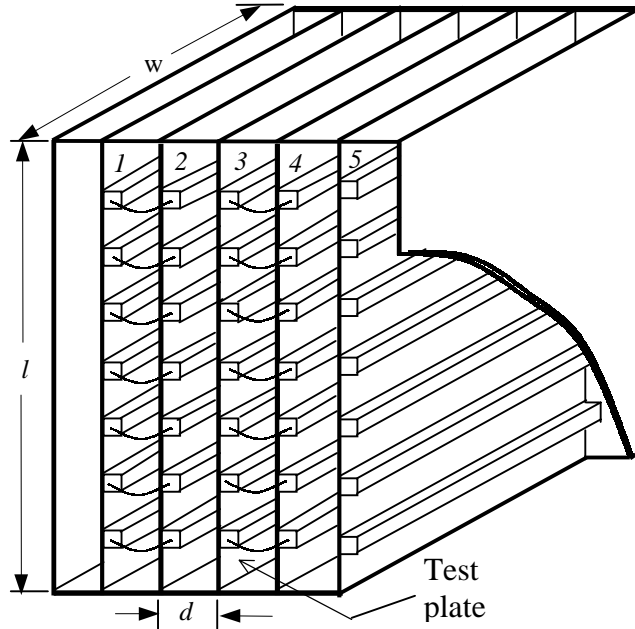


Figure 2 - Schematic view of experimental setup.

Experiments were performed varying the distance between plates and the total heat generation Q , set the same for all plates during the tests. The distance between plates was ranged from 2 to 4cm, what corresponds to ratio ($L = l/d$) between 9 and 18, and the total heat generation per plate from 20 to 60W. The Rayleigh number was ranged from $1 \cdot 10^4$ to $8 \cdot 10^5$.

Temperature differences among the plates (in the x direction) were verified by embedding, in each plate, thermocouples to the protruding heat source positioned in row 4.

Figure (3) represents a test plate. The symbols \times and \circ indicate the points of the protuberance surface and plate surface where temperature was measured, respectively. The measurements were done at plate 3. Symbol \circ indicates air temperature measurement at the exit and at the entrance of the channel formed by plates 3 and 4. Steady-state was attained about one hour after the beginning of the tests.

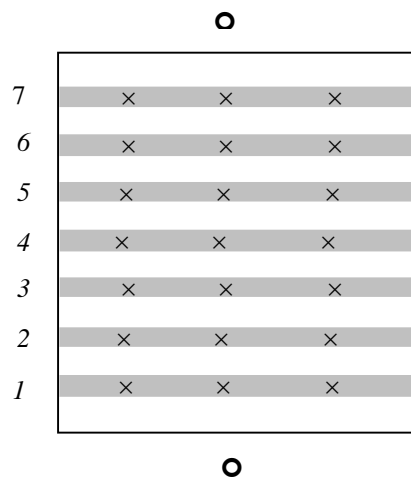


Figure 3 - Temperature sensors location at test plate.

4. RESULTS AND DISCUSSIONS

Figures (4) and (5) show temperature excess profiles for several values of total heat generation rate per plate, and distance between plates equal to 2 cm and 4 cm. The temperature excess, ΔT , is defined as the difference between the air inlet temperature, T_o , and the heat source temperature, T_p .

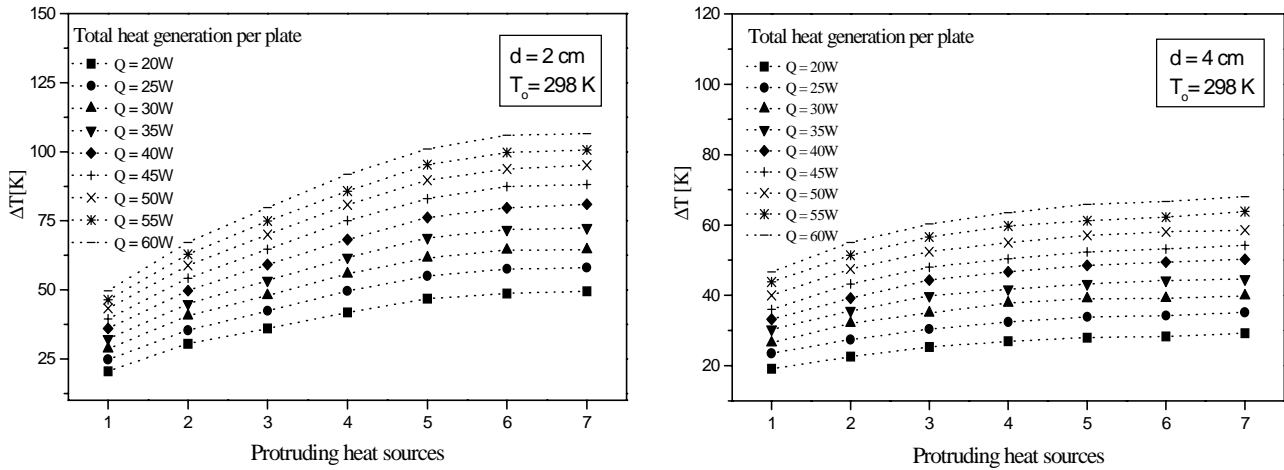


Figure 4 - Temperature excess profiles - $d = 2$ cm. Figure 5 - Temperature excess profiles - $d = 4$ cm.

By comparing Figs. (4) and (5), it can be noticed that the temperature gradient along the plate becomes less accentuated as the distance between plates increases. From Fig. (4) it can be observed that for the smallest plate spacing, 2cm, the temperature profile is almost linear from the second to the fifth element for all values of total heat generation rate. This behavior was described by Kelkar and Choudhury (1993), who numerically investigated the fully developed natural convection in a vertical channel with surface mounted heat generation blocks, equally spaced. When this regime is established, the flow pattern around each module is the same, and the temperature difference between correspondent points in adjacent modules is constant. In the present work, the elements are equally spaced, they have the same heat generation rate, and, in the periodical regime, the temperature must increase linearly, what is verified in Fig. (4).

Figure (6) shows isotherms for the spacing plate to plate equal to 2cm and total heat generation rate per plate equal to 25W. For convenience, the channel is presented in the horizontal direction.

The isothermal lines shown in Fig (6) are crowded on the surfaces that are parallel to the main flow direction and near the protrusions bottom corner (remembering that the channel are presented in the horizontal direction). This means that the heat transfer rates are higher in these regions.

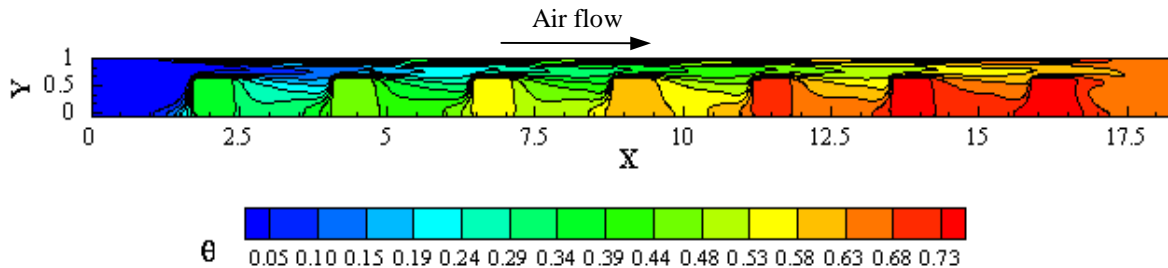


Figure 6 - Isotherms - $d = 2$ cm - $Q = 25$ W - $Ra_d = 5 \times 10^4$ - $u_o = 0,11$ m/s.

Figures (7) and (8) show streamlines for the same values of total heat generation rate and distance between plates. It is observed that recirculation regions are formed between the protrusions, and that the flow pattern around each protrusion is almost the same in the region between the second and the fifth protrusions. This periodicity was also observed experimentally in

the temperature field for the distance of 2cm. A more accentuated recirculation is noticed near the channel exit.

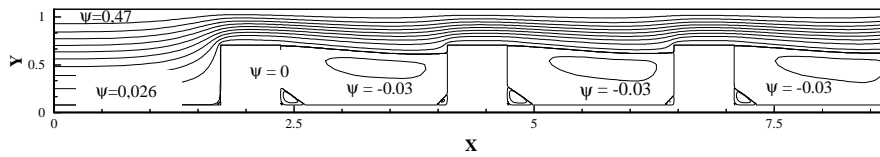


Figure 7 - Streamlines between the channel entrance and the fourth protrusion - $Q = 25W$ - $d = 2cm$.

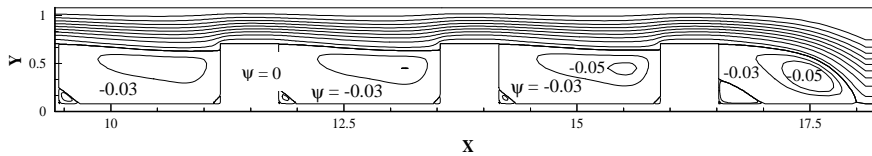


Figure 8 - Streamlines between the fourth and the last protrusion - $Q = 25W$ - $d = 2cm$.

In Fig. (9) it is compared numerical and experimental values of dimensionless temperature excess and Nusselt number. The experimental results are indicated by bars whose dimensions represent, approximately, the uncertainty range of the experimental results. To determine the experimental Nusselt number values, the heat transferred by conduction from each protrusion to the plate was numerically determined, and this values was discounted from the total heat generation of each element, then obtaining the heat transferred by convection, Q_c , in each element. Finally, the Nusselt number was calculated by the expression

$$Nu_{m_{exp}} = \frac{Q_c d}{(T_p - T_o)_{exp} A_c k_f} \quad (8)$$

where A_c is the element surface area.

As it can be notice from Figs. (9) and (10), good agreement was observed between numerical and experimental results for both temperature and Nusselt Number. The maximum discordance between numerical and experimental results is found to be about 6% for temperature excess and about 8% for Nusselt number.

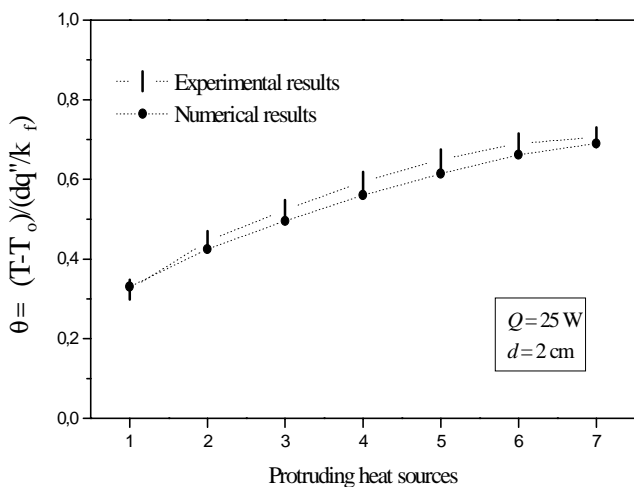


Figure 9 - Numerical and experimental values of dimensionless temperature excess.

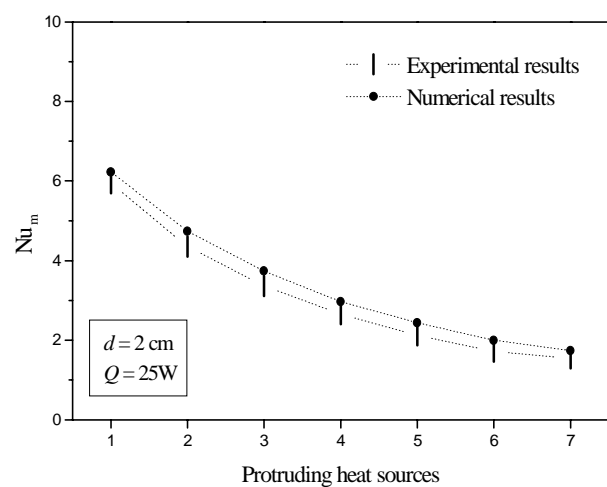


Figure 10 - Numerical and experimental values of Nusselt number.

Figure (11) shows isotherms for the distance between plates equal to 2,5cm and total heat generation rate per plate equal to 25W.

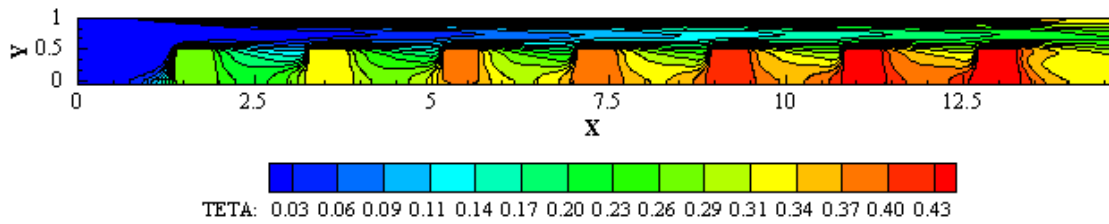


Figure 11 - Isotherms - $d = 2,5\text{cm}$ - $Q = 25\text{W}$ - $Ra_d = 1 \times 10^5$ - $u_o = 0,143\text{m/s}$.

By comparing Fig. (6), where it is presented isotherms for the distance $d=2\text{cm}$, and Fig. (11), it can be noticed a longer unheated fluid length for the distance of $2,5\text{cm}$. As in Fig. (6), the isothermal lines presented in Fig (11) are densely distributed on the surfaces that are parallel to the main flow direction and near the protrusions bottom corners.

Figs. (12) and (13) show streamlines for the same values of total heat generation and distance between plates. It can be noticed that, as already observed for distance between plates equal to 2cm , the flow pattern between the second and sixth protrusions is very similar, but significant differences can be noticed in the flow patterns in the channel exit.

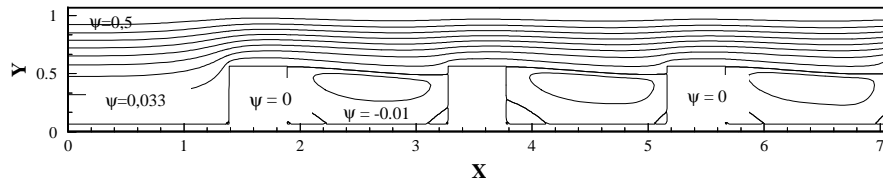


Figure 12 - Streamlines between the channel entrance and the fourth protrusions - $Q=25\text{W}$ - $d=2,5\text{cm}$.

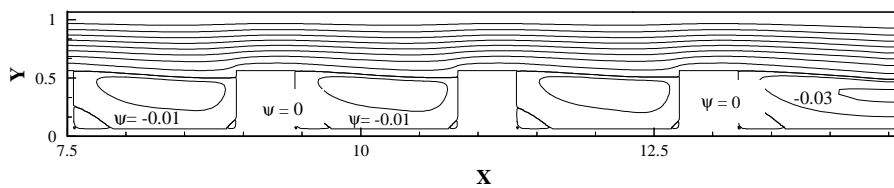


Figure 13 - Streamlines between the fourth and the last protrusions - $Q = 25\text{W}$ - $d = 2,5\text{cm}$.

Isotherms for the distance between plates equal to $3,5\text{cm}$ and total heat generation rate per plate equal to 35W are presented in Fig. (14).

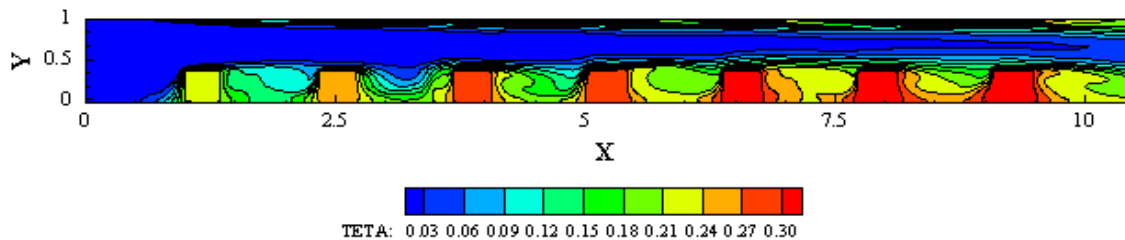


Figure 11 - Isotherms - $d = 3,5\text{cm}$ - $Q = 25\text{W}$ - $Ra_d = 4 \times 10^5$ - $u_o = 0,184\text{m/s}$.

Comparing the isotherms presented in Fig. (14) with the isotherms presented for the distances 2cm and $2,5\text{cm}$, it can be noticed that the length of unheated fluid is even longer. This means that as the distance between plates increases, the channel flow becomes very similar to the flow along a plate in an infinite medium. It can be observed also that the induced flow rates in the channel increases significantly as the plates becomes more separated.

In Fig. (15) and (16) it is compared numerical and experimental values of dimensionless temperature excess for total heat generation rate per plate equal to 25W and for the values of distances between plates equal to 2,5cm and 3,5cm.

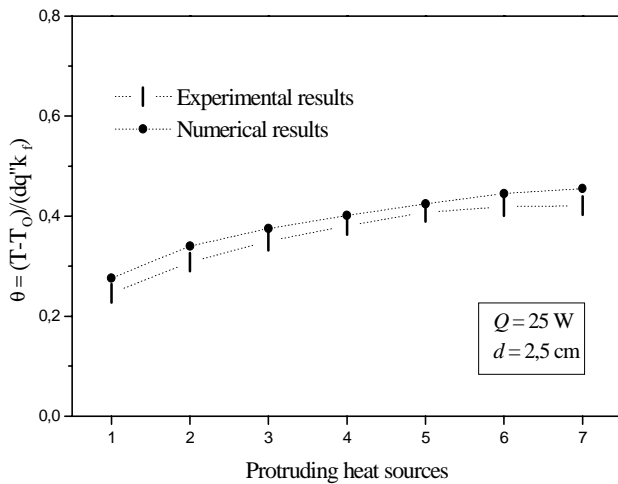


Figure 15 - Dimensionless temperature excess Profiles - $Q = 25 \text{ W}$ - $d = 2,5 \text{ cm}$.

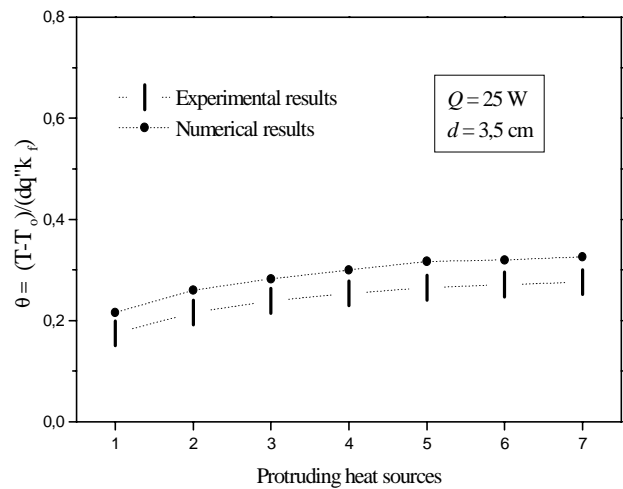


Figure 16 - Dimensionless temperature excess Profiles - $Q = 25 \text{ W}$ - $d = 2,5 \text{ cm}$.

Comparing Figs. (15) and (16), it can be notice that in both cases, $d=2,5\text{cm}$ and $d=3,5\text{cm}$, the temperature profile was well reproduced numerically. The concordance between numerical and experimental results is better for the smaller distances between plates.

In Fig. (17) and (18) it is compared numerical and experimental values of dimensionless temperature excess for the values of total heat generation rate per plate equal to 10W and 45W and plate spacing equal to 2,5cm. It can be observed that the curves of temperature profiles are very similar for the values of total heat generation of 10W and 45W.

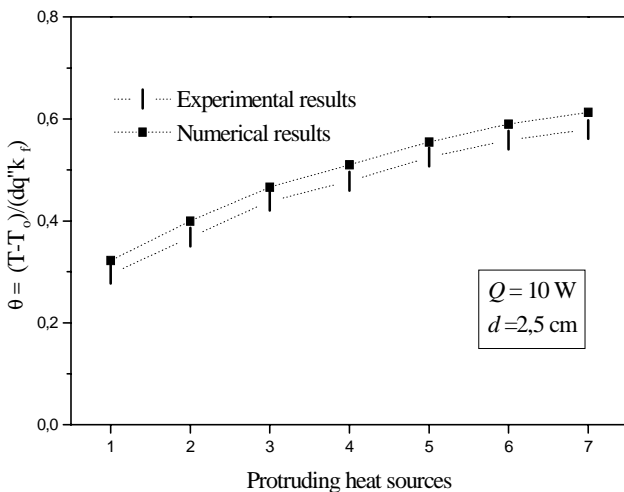


Figure 17 - Dimensionless temperature excess Profiles - $Q = 10 \text{ W}$ - $d = 2,5 \text{ cm}$.

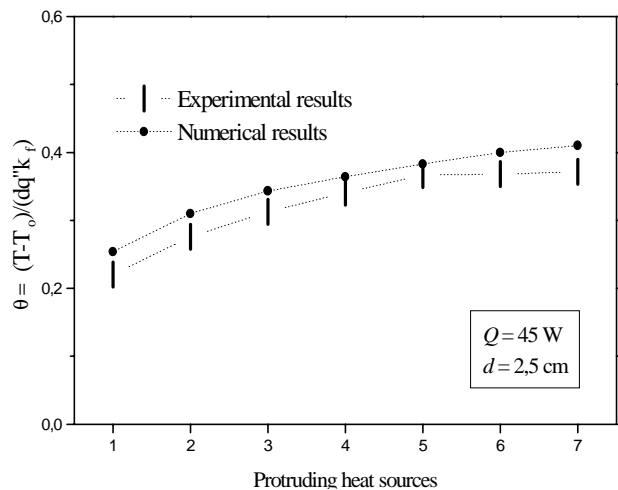


Figure 18 - Dimensionless temperature excess Profiles - $Q = 45 \text{ W}$ - $d = 2,5 \text{ cm}$.

The maximum differences between numerical and experimental are about 10%. For the heat generation of 45W, the maximum difference between numerical and experimental results was verified at channel exit, what can be a consequence of the radiation heat transfer, which is expected to be more intense in the last element.

5. CONCLUSIONS

Natural convection heat transfer from an array of vertical, parallel plates, forming open channels containing heated protruding elements attached to one of the walls, was analyzed both numerically and experimentally. The obtained results suggest the following conclusions:

- The experimental results shown that the shape of the curves of temperature excess along the plate presents slight variation with the increase in the heat rate dissipated per plate. However, the temperature gradient along the plate becomes less accentuated;
- For the smallest plate spacing, 2cm, it was verified that the flow is periodically fully developed between the second and the fifth protruding heat source, i. e., the flow pattern is almost the same around each element, and the temperature variation between correspondent points in adjacent elements is constant;
- Good agreement between numerical and experimental results was verified. The differences between numerical and experimental results ranged from 6% to 14%. The highest difference was verified for the highest values of distances between plates and power dissipated per plate;
- Increasing the distance between plates causes longer lengths of unheated fluid, approaching the condition of a plate in an infinite medium. Isotherms distribution show higher heat transfer rates at the protrusions bottom corners and the faces parallel to the main flow direction.

6. ACKNOWLEDGMENTS

To FAPESP for the financial support and to CENAPAD-SP for computer support.

7. REFERENCES

- Behnia, M., Nakayama, W., 1998, "Numerical Simulation of Combined Natural Convection-Conduction Cooling of Multiple Protruding Chips on a Series of Parallel Substrates", Proceedings of InterSociety Conference on Thermal Phenomena.
- Elenbaas, W., 1942, "Heat Dissipation of Parallel Plates by Free Convection", Physical, Vol. 9, pp. 1-28,.
- Fujii, M., Gima, S., Tomimura, T., Zhang, Z., 1996, "Natural Convection to Air From an Array of Vertical Parallel Plates With Discrete and Protruding Heat Sources", International Journal of Heat and Fluid Flow, Vol. 17, pp. 483-490.
- Incropera, F. P., 1988, "Convection Heat Transfer in Electronic Equipment Cooling", Journal of Heat Transfer, Vol.110, No.43, pp.1097-1111.
- Kelkar, K. M., Choudhury, D., 1993, Numerical Prediction Of Periodically Fully Developed Natural Convection in a Vertical Channel With Surface Mounted Heat Generating Blocks. International Journal of Heat and Mass Transfer, V.36, N.5, P.1133-1145.
- Patankar, S. V., Liu, C. H., Sparrow, E. M., 1977, "Fully Developed Flow and Heat Transfer in Ducts Having Streamwise-Periodic Variations of Cross-sectional Area", Journal of Heat Transfer, Vol.99.
- Patankar, S. V., 1990, "Numerical Heat Transfer and Fluid Flow", New York Publishing Co, 1980.
- Peterson, G. P., Ortega, A. "Thermal Control of Electronic Equipment and Devices". Advances in Heat Transfer, Vol.20, pp.181-314.
- Viswamula, P., Amin, M. R., 1995, "Effects of Multiple Obstructions on Natural Convection Heat Transfer in Vertical Channels", International Journal of Heat and Mass Transfer, Vol. 18, No. 11, pp.2039-2046.
- Van Doormaal, J. P., Raithby, G. D., 1984, "Enhancements of the Simple Method for Predicting Incompressible Fluid Flows", Numerical Heat Transfer, Vol.7, pp.147-163, 1984.

